Anisotropic Flow and Jet Quenching in Ultrarelativistic U+U Collisions

Ulrich Heinz and Anthony Kuhlman
Department of Physics, The Ohio State University, Columbus, Ohio 43210, USA
(Received 16 November 2004; published 6 April 2005)

Full-overlap U + U collisions provide significantly larger initial energy densities at comparable spatial deformation, and significantly larger deformation and volume at comparable energy density, than semi-central Au + Au collisions. We show quantitatively that this provides a long lever arm for studying the hydrodynamic behavior of elliptic flow in much larger and denser collision systems and the predicted nonlinear path-length dependence of radiative parton energy loss.

DOI: 10.1103/PhysRevLett.94.132301 PACS numbers: 25.75.-q, 12.38.Mh, 12.38.Qk

Two major discoveries made in relativistic Au + Au collisions at the Relativistic Heavy Ion Collider (RHIC) are the large magnitude and almost ideal fluid dynamical behavior of the elliptic flow, and the observation of a strong suppression of high-p_T particle production and jet quenching [1,2]. Combined with a range of other observations, they led several authors to claim creation of a thermalized quark-gluon plasma (QGP) in these collisions [3–6]. While this question is still being extensively discussed by the wider RHIC community, it is clear that, even if the answer is positive, we have only just scratched the surface of understanding the properties of this QGP.

In this Letter we address two important open questions and suggest that experiments studying full-overlap U + U collisions can contribute decisively to answering them, by exploiting the unique differences between the side-on-side and edge-on-edge configurations when colliding significantly deformed nuclei. The first concerns the observed almost ideal fluid dynamical behavior of the "elliptic flow," described by the second Fourier coefficient v_2 of the azimuthal momentum distribution of emitted particles. As noted in [7], the final momentum anisotropy v_2 is driven by the initial spatial eccentricity ϵ_x of the nuclear overlap region via anisotropic pressure gradients. Systematic studies of v_2 at midrapidity in Au + Au and Pb + Pb collisions of varying centrality at the Alternating Gradient Synchrotron (AGS), Super Proton Synchrotron (SPS), and RHIC [8,9] show that the ratio v_2/ϵ_x scales with the charged multiplicity density per unit transverse area, $\frac{1}{S}\frac{dN_{\rm ch}}{dy}$, which is proportional to the initial entropy density s_0 of the reaction zone. A similar scaling is seen when studying v_2/ϵ_x as a function of rapidity in minimum bias Au + Au collisions at RHIC [10–12]. Predictions from ideal fluid dynamics [13] agree with the data only at the top RHIC energy, in almost central Au + Au collisions, and at midrapidity, where the highest initial entropy densities are created. As one moves to more peripheral collisions, lower collision energies, or away from midrapidity, the measured elliptic flow begins to increasingly fall below the ideal fluid limit. According to Figure 25 in [9], the data do not seem to approach the ideal fluid limit gradually, but follow a trend which seems to *cross* the hydrodynamic curve near $\frac{1}{S}\frac{dN_{\rm ch}}{dy} \approx 25/\mathrm{fm}^2$ [14]. This is unexpected since the ideal fluid value for v_2/ϵ_x is an upper limit which should not be exceeded [15]. It is therefore very important to check that at larger values of $\frac{1}{S}\frac{dN_{\rm ch}}{dy}$ the data indeed settle down on the hydrodynamic prediction. If they do not, this would imply a stiffer QGP equation of state than so far assumed since the hydrodynamic value of v_2/ϵ_x increases with the speed of sound [7]. With Au + Au collisions the only possibility to further raise $\frac{1}{S}\frac{dN_{\rm ch}}{dy}$ is to increase the collision energy, which requires waiting for the Large Hadron Collider (LHC). We show here that with full-overlap U + U collisions at top RHIC energy in edge-on-edge geometry, one can increase $\frac{1}{S}\frac{dN_{\rm ch}}{dy} \sim s_0$ by $\approx 55\%$, to values around 40 fm^2. This is a larger gain than between Au + Au collisions at impact parameters $b = 0$ and $b \simeq 10$ fm.

The second major open question is which mechanism is responsible for the large observed energy loss of fast partons travelling through the dense medium. Fits of the energy loss data at RHIC with a theory based on non-Abelian radiative energy loss in a thermalized, color deconfined medium [16] work well and yield initial energy densities consistent with those required for a successful hydrodynamic description of the elliptic flow [4]. However, the theory makes the specific prediction [17] that the dependence of the energy loss on the path length through the dense medium should be nonlinear, and this has not yet been tested. Experiments show that in semiperipheral Au + Au collisions fast partons travelling through the medium in the direction perpendicular to the reaction plane lose more energy than partons passing through it in the shorter in-plane direction [18]. While this does prove path-length dependence of the energy loss, existing analyses cannot distinguish between different types of path-length dependences. The rather small size of the fireball created in semiperipheral Au + Au collisions does not provide much of a path-length difference between the in-plane and out-of-plane directions, thus limiting the resolving power. We show here that this situation improves

dramatically in full-overlap U + U collisions whose initial overlap zone in the side-on-side configuration is about twice as large as that created in semiperipheral Au + Au collisions of similar eccentricity, thereby increasing by more than 100% both the absolute value of the radiative energy loss and its difference between in-plane and out-of-plane directions.

Uranium-uranium collisions have been proposed before [13,19,20]. The present work goes beyond these studies by providing quantitative calculations of the distributions of multiplicity and spatial eccentricity in full-overlap U + U collisions and by presenting semiquantitative estimates of the energy loss of fast partons as a function of their azimuthal emission angle. Our calculations demonstrate conclusively that a meaningful research program with full-overlap U + U collisions is experimentally feasible, and that it provides a strong lever arm for studying the hydrodynamic behavior of anisotropic flow and the nonlinear path-length dependence of non-Abelian radiative parton energy loss as predicted by QCD.

We compute the initial entropy production in the $z = 0$ transverse plane with a Glauber ansatz [21] where a fraction α is taken to scale with the tranverse density $n_{\rm w}(\boldsymbol{r}_\perp)$ of wounded nucleons while the remainder scales with the density of binary collisions $n_{\rm b}(\boldsymbol{r}_\perp)$:

$$s(\boldsymbol{r}_\perp;\Phi) = \kappa_s[\alpha n_{\rm w}(\boldsymbol{r}_\perp;\Phi) + (1-\alpha)n_{\rm b}(\boldsymbol{r}_\perp;\Phi)]. \quad (1)$$

We consider only $b = 0$ collisions with full nuclear overlap, by using the two forward and backward zero degree calorimeters to select high-multiplicity events with essentially no spectator nucleons along the beam directions. The collision configuration is then completely controlled by the polar angle Φ between the beam direction and the symmetry axis of one of the two deformed U nuclei since full overlap requires the uranium axes to be coplanar while their angles with the beam axis satisfy $\Phi_1 = \pm\Phi_2$ (see illustration in Fig. 3 below) [22].

We use a Woods-Saxon form for the uranium density with $R(\theta) = (6.8\ \text{fm})(0.91 + 0.26\cos^2(\theta))$ for the nuclear radius as a function of the polar angle θ relative to the nuclear symmetry axis and with surface thickness parameter $\xi = 0.54$ fm. This gives $R_\parallel = 7.94$ fm and $R_\perp = 6.17$ fm, with a ratio $R_\parallel/R_\perp = 1.29$ [13,20,23]; it ignores the hexadecupole moment of the U nucleus [23]. The normalization κ_s in Eq. (1) is adjusted to obtain a central entropy density in $b = 0$ Au + Au collisions of $s_0 = 117\ \text{fm}^{-3}$ at proper time $\tau_0 = 0.6\ \text{fm}/c$; after hydrodynamic evolution [13,21] this reproduces the charged particle multiplicity measured at midrapidity in such collisions at $\sqrt{s_{NN}} = 200$ GeV [24]. α in Eq. (1) is fitted to the centrality dependence of the charged particle multiplicity in Au + Au collisions at $\sqrt{s_{NN}} = 200$ GeV [24], by assuming that particle production is proportional to the total entropy in the transverse plane: $\frac{dN_{\rm ch}}{d\eta}(b) \propto \int d^2r_\perp s(\boldsymbol{r}_\perp;b)$. The resulting fit parameter $\alpha = 0.75$ is consistent with results obtained in Ref. [25] using a different form of parametrization.

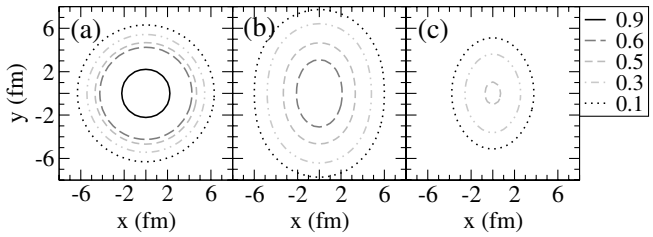

FIG. 1. Entropy density contours for full-overlap U + U collisions with $\Phi = 0$ (a) and $\Phi = \frac{\pi}{2}$ (b), and for $b = 7$ fm Au + Au collisions (c). Lines show specified fractions of the peak entropy density $s_0^{\rm UU} = 167\ \text{fm}^{-3}$ in $\Phi = 0$ U + U collisions.

After fitting the Glauber model parameters to Au + Au data at 200A GeV, we can predict the particle multiplicities for U + U collisions at the same energy. Because of the binary collision component, particle production in full-overlap U + U collisions varies by almost 15% between the side-on-side and edge-on-edge configurations (see Fig. 3), even though the number of wounded nucleons is almost constant [26].

Figure 1 presents contour plots of the initial entropy distribution in the transverse plane. The left two panels show the profiles expected for central U + U collisions with $\Phi = 0$ and $\Phi = \frac{\pi}{2}$, respectively. The side-on-side configuration produces a substantial out-of-plane deformation, whereas the edge-on-edge configuration has a much higher peak entropy density, due to the larger binary collision component and the smaller transverse overlap area. The initial eccentricity of the reaction zone

$$\epsilon_x(\Phi) = \frac{\int d^2r_\perp(y^2 - x^2)s(\boldsymbol{r}_\perp;\Phi)}{\int d^2r_\perp(y^2 + x^2)s(\boldsymbol{r}_\perp;\Phi)} \quad (2)$$

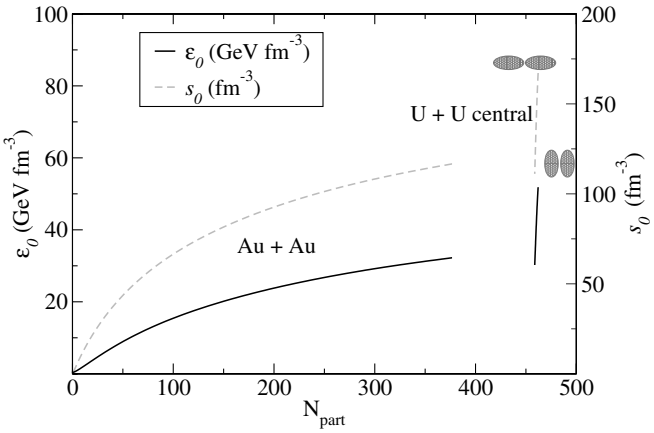

FIG. 2. Peak energy density (left ordinate) and entropy density (right ordinate) as a function of the number of participants, for Au + Au collisions of varying impact parameter and full-overlap U + U collisions.

ranges from $\epsilon_x = 0$ in the edge-on-edge configuration to $\epsilon_x = 0.25$ in the side-on-side case. The latter value is almost as large as for $b = 7$ fm Au + Au collisions [Fig. 1(c)], but in this case the overlap region covers less than half the area, and the peak entropy density is about 25% smaller. Averaging the full-overlap U + U collisions over all angles Φ gives $\langle \epsilon_x \rangle \approx 0.13$, showing that the average reaction zone retains more than 50% of its maximum deformation.

Figure 2 compares the peak energy and entropy densities in Au + Au and central U + U collisions. All curves refer to time $\tau_0 = 0.6$ fm/c and $\sqrt{s_{NN}} = 200$ GeV. The conversion of entropy to energy density assumes an ideal quark-gluon gas equation of state. The maximum peak energy density in central U + U is seen to be about 62% larger than that in the most central Au + Au collisions. This gives a large lever arm to probe the approach to ideal hydrodynamic behavior of v_2.

Figure 3 shows the charged multiplicity distribution of full-overlap U + U collisions. To compute it we introduce event-by-event multiplicity fluctuations at fixed angle Φ via the probability density [25]

$$\frac{dP}{dnd\Phi} = A \exp\left\{-\frac{(n - \bar{n}(\Phi))^2}{2a\bar{n}(\Phi)}\right\}, \tag{3}$$

with $a = 0.6$ [25], and integrate over Φ. Here n is shorthand for $\frac{dN_{ch}}{dy}$. The average multiplicity $\bar{n}(\Phi)$ is computed from the transverse integral over Eq. (1), using the appropriate proportionality constant. The resulting multiplicity distribution in Fig. 3 exhibits Jacobian peaks near $\Phi = 0$ and $\Phi = \frac{\pi}{2}$ since $d\bar{n}/d\Phi$ is smaller for angles near 0° and 90° than for intermediate ones. Of course, Fig. 3 represents the ideal case of strictly rejecting spectators on either side of the collision point [22].

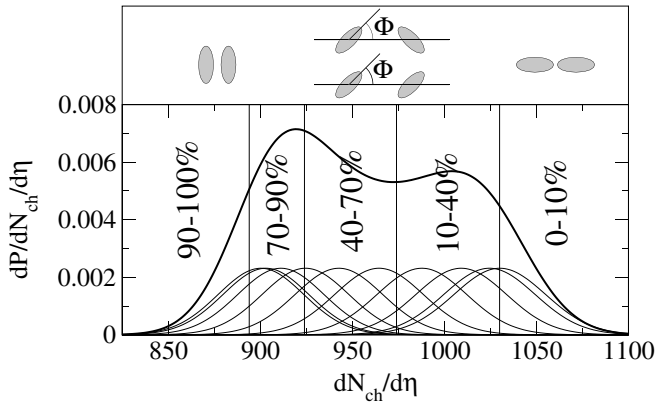

FIG. 3. Multiplicity distribution for full-overlap U + U collisions. The Gaussian curves at the bottom show individual distributions for fixed angles Φ from 0° (right) to 90° (left), in 10° increments. The vertical lines cut the area under the curve according to the listed percentages.

This multiplicity distribution can be converted to a distribution of eccentricities via

$$\left.\frac{dP}{d\epsilon_x}\right|_{n_0}^{n_1} = \frac{B}{d\epsilon_x/d\Phi} \int_{n_0}^{n_1} dn \exp\left\{-\frac{(n - \bar{n}(\Phi))2}{2a\bar{n}(\Phi)}\right\}. \tag{4}$$

Distributions corresponding to the cuts shown in Fig. 3 are plotted in Fig. 4. One sees that by cutting on multiplicity one can effectively select the initial eccentricity, especially near the upper and lower end of the multiplicity distribution.

We close by estimating the radiative energy loss, ΔE, of a fast parton moving through the fireball medium. Our goal is not an accurate calculation of this quantity, which would require a more sophisticated treatment, but a qualitative comparison of the additional reach provided by central U + U collisions compared to Au + Au. Following Ref. [2], we therefore consider the figure of merit

$$t \equiv \int_{\tau_0}^{\infty} d\tau \rho(\boldsymbol{r}_\perp(\tau), \tau)(\tau - \tau_0) \tag{5}$$

as a measure expected to be roughly proportional to the energy loss ΔE. $\boldsymbol{r}_\perp(\tau)$ denotes the parton trajectory, and $\rho(\boldsymbol{r}_\perp(\tau), \tau)$ is the total parton density in the medium.

Figure 5 compares the energy loss for inward-moving partons produced near the edge [27] of the fireball (see inset) for Au + Au and full-overlap U + U collisions. The top panel (labeled t_0) assumes that the parton density does not change while the parton passes through the fireball; the bottom panel accounts for dilution of the density by longitudinal expansion using $\rho(\boldsymbol{r}_\perp, \tau) = \frac{\tau_0}{\tau}\rho(\boldsymbol{r}_\perp, \tau_0)$. The energy loss is calculated as a function of source eccentricity ϵ_x, and we compare it for partons emitted into ($\phi = 0$) and perpendicular to the reaction plane ($\phi = \frac{\pi}{2}$) [28]. In Au + Au collisions, changing the eccentricity in order to study the path-length dependence of energy loss requires going to more peripheral collisions which produce smaller fireballs. In full-overlap U + U collisions, the eccentricity can be increased without decreasing the fireball size (although the density decreases somewhat). Were it not for the dilution of the density due to longitudinal expansion, this would in fact lead to *larger* energy loss for out-of-plane

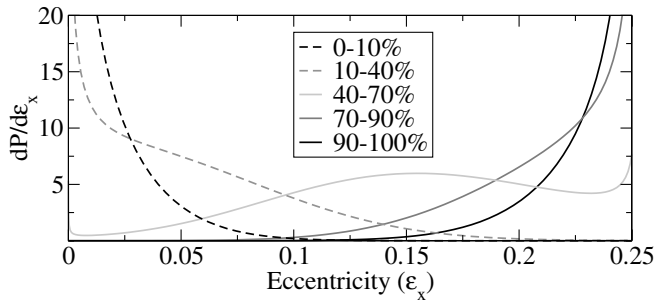

FIG. 4. Eccentricity distributions corresponding to the multiplicity cuts shown in Fig. 3.

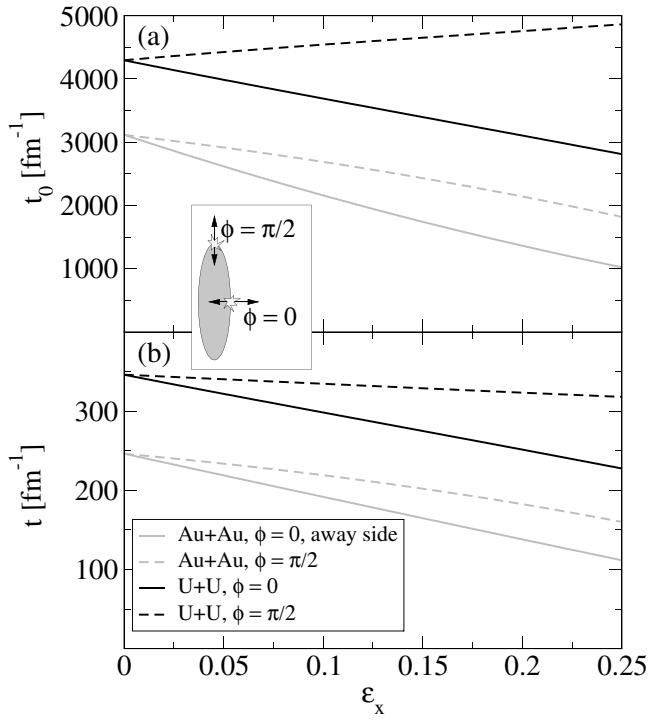

FIG. 5. Energy loss as a function of eccentricity for U + U (black) and Au + Au collisions (gray), assuming constant density (a) and dilution via longitudinal expansion (b). See text for discussion.

partons emitted from side-on-side collisions compared to edge-on-edge collisions (dashed line in Fig. 5(a)]. When longitudinal expansion is included (bottom panel), the energy loss for out-of-plane emitted partons from U + U collisions is still almost independent of eccentricity, whereas the in-plane energy loss decreases by about 35% between edge-on-edge and side-on-side collisions. In Au + Au collisions the energy loss decreases with increasing ϵ_x in both cases (by 35% and 55%, respectively), leading to an overall loss of discriminating power on its path-length dependence. For the largest eccentricities, the *difference* in energy loss between out-of-plane and in-plane emission in U + U is more than twice that which can be achieved in Au + Au collisions. The *total* energy loss is also larger by up to a factor 2, causing significant jet quenching and reduced particle production up to much larger p_T values in full-overlap U + U collisions than in Au + Au collisions.

We thank R. Furnstahl and I. Tornes for helpful technical comments and acknowledge support by the U.S. DOE under contract no. DE-FG02-01ER41190.

[1] Most of these developments can be found in the proceedings of the last three Quark Matter Conferences: *Quark Matter 2001*, edited by T. J. Hallman *et al.* [Nucl. Phys. A 698, 3c (2002)]; *Quark Matter 2002*, edited by H. Gutbrod, J. Aichelin, and K. Werner [Nucl. Phys. A 715, 3c (2003)]; *Quark Matter 2004*, edited by H. G. Ritter and X.-N. Wang [J. Phys. G 30, S633 (2004)].

[2] For theoretical reviews see M. Gyulassy, I. Vitev, X.-N. Wang, and B.-W. Zhang, in *Quark-Gluon Plasma 3*, edited by R. C. Hwa and X.-N. Wang (World Scientific, Singapore, 2004), p. 123; A. Kovner and U. A. Wiedemann, *ibid.*, p. 192; P. F. Kolb and U. Heinz, *ibid.*, p. 634.

[3] U. Heinz, Nucl. Phys. A **721**, 30c (2003).

[4] M. Gyulassy, nucl-th/0403032.

[5] E. V. Shuryak, Nucl. Phys. A **750**, 64 (2005).

[6] B. Müller, Nucl. Phys. A **750**, 84 (2005).

[7] J. Y. Ollitrault, Phys. Rev. D **46**, 229 (1992).

[8] STAR Collaboration, C. Adler *et al.*, Phys. Rev. C **66**, 034904 (2002).

[9] NA49 Collaboration, C. Alt *et al.*, Phys. Rev. C **68**, 034903 (2003).

[10] PHOBOS Collaboration, B. B. Back *et al.*, Phys. Rev. Lett. **89**, 222301 (2002).

[11] T. Hirano, Phys. Rev. C **65**, 011901(R) (2002).

[12] U. Heinz and P. F. Kolb, J. Phys. G **30**, S1229 (2004).

[13] P. F. Kolb, J. Sollfrank, and U. Heinz, Phys. Rev. C **62**, 054909 (2000).

[14] Other more technical roots of this tendency were suggested by M. Miller and R. Snellings, nucl-ex/0312008.

[15] U. Heinz and P. F. Kolb, Nucl. Phys. A **702**, 269 (2002).

[16] I. Vitev and M. Gyulassy, Phys. Rev. Lett. **89**, 252301 (2002).

[17] R. Baier, Yu. L. Dokshitzer, A. H. Mueller, S. Peigne, and D. Schiff, Nucl. Phys. B **483**, 291 (1997); R. Baier, Yu. L. Dokshitzer, A. H. Mueller, S. Peigne, and D. Schiff, *ibid.* **484**, 265 (1997).

[18] STAR Collaboration, J. Adams *et al.*, Phys. Rev. Lett. **93**, 252301 (2004).

[19] Bao-An Li, Phys. Rev. C **61**, 021903(R) (2000).

[20] E. V. Shuryak, Phys. Rev. C **61**, 034905 (2000).

[21] P. F. Kolb, U. Heinz, P. Huovinen, K. J. Eskola, and K. Tuominen, Nucl. Phys. A **696**, 197 (2001).

[22] Here we do not attempt to estimate the smearing effects from collisions with small nonzero impact parameters or with symmetry axes that are not exactly coplanar. While they can be minimized by imposing stringent experimental cuts, they cannot be completely avoided. Their study requires a multidimensional simulation in the space defined by the impact parameter b and the two Euler angles associated with the relative orientation of the U nuclei; we postpone this for a longer publication.

[23] A. Bohr and B. R. Mottelson, *Nuclear Structure* (Benjamin, New York, 1969), Vol. II.

[24] PHOBOS Collaboration, B. B. Back *et al.*, Phys. Rev. C **65**, 061901 (2002).

[25] D. Kharzeev and M. Nardi, Phys. Lett. B **507**, 121 (2001).

[26] For side-on-side collisions the fraction of surface nucleons passing through without scattering is slightly larger.

[27] The ''edge'' is defined as the parton density contour corresponding to 10% of the peak value.

[28] We only consider partons created at the specific points shown in the inset of Fig. 5. A more quantitative study will require averaging over all possible production points.